Articles

Escherichia coli Primase Zinc Is Sensitive to Substrate and Cofactor Binding†

L. Powers‡ and Mark A. Griep*,§

National Center for the Design of Molecular Function, Department of Electrical and Computer Engineering, Utah State University, Logan, Utah 84322-4630, and Department of Chemistry and the Center for Biotechnology, University of Nebraska, Lincoln, Nebraska 68588-0304

Received December 29, 1998

ABSTRACT: The ligation state of the single zinc site in primase from *Escherichia coli* changes when various substrates and cofactors are added alone or in combination as determined by X-ray absorption spectroscopy. X-ray absorption spectroscopy (XAS) provides information about the local structure (∼5 Å) of atoms surrounding the metal and has been widely used to characterize metalloproteins. The zinc site in native primase and in primase bound to low (30 mM) magnesium acetate was found to be tetrahedrally ligated by three sulfurs at an average distance of 2.36 ± 0.02 Å and one histidine nitrogen located at a distance of 2.15 ± 0.03 Å. When ATP, ATP and $(dT)_{17}$, or ATP, low magnesium acetate and $(dT)_{17}$ was added to primase, one (or two) additional nitrogen/oxygen ligands were coordinated to the zinc together with the histidine nitrogen at an average distance of 2.15 ± 0.03 Å. These additional ligands are likely from adjacent phosphates from ATP. Another structure was observed for the primase-$(dT)_{17}$ complex in which an additional nitrogen/oxygen ligand likely from the phosphate backbone together with the histidine nitrogen was located at a significantly shorter average distance of 2.05 ± 0.03 Å. High magnesium acetate (300 mM) completely inactivates primase in a reversible manner such that the region near the zinc ligands becomes accessible to proteolytic digestion [Urlacher, T. M., and Griep, M. A. (1995) *Biochemistry 34*, 16708−16714]. In this inactive complex, additional oxygen/nitrogen ligands from acetate as well as the histidine nitrogen are located at a distance of 2.20 ± 0.03 Å from the zinc site. To test whether the catalytic magnesium was binding within ∼5 Å of the zinc, we incubated primase with high (300 mM) manganese acetate. The functional properties of magnesium and manganese are similar, but the larger atomic number of manganese enhances the X-ray backscattering, making it possible to identify. Since no significant difference was observed from the manganese-incubated sample, the catalytic metal-binding site is likely located >5 Å from the zinc. These studies clearly show that primase zinc ligation changes upon binding substrates.

Primase is the single-stranded DNA-dependent RNA polymerase that initiates DNA polymer synthesis once for the leading strand DNA polymerase and multiple times for the lagging strand DNA polymerase (*1*, *2*). Leading strand synthesis is initiated by primase at the replication origin after origin-specific proteins and enzymes have opened the duplex DNA at that site. Once opened by DnaB helicase, two replication forks moving in opposite directions each create two antiparallel DNA template single strands. At each replication fork, the leading strand template is continually replicated by the leading strand half of the dimeric DNA polymerase which had been initiated at the origin (*3*, *4*). However, the lagging strand cannot be continually replicated because it is in the wrong direction for the unidirectional DNA polymerase. As a result, synthesis on the lagging strand has to be initiated by the unidirectional primase. This occurs once every 500−2000 nucleotides. The 11 ± 1 nucleotide RNA polymer is elongated by the lagging strand half of the DNA polymerase for the remaining 500−2000 nucleotides. In an *Escherichia coli* lagging strand DNA synthesis system, the initiating and rate-limiting event was shown to involve primer synthesis (*5*, *6*). In a study of primase activity alone, its rate-limiting step was identified as either formation of the first phosphodiester bond or, more likely, a step preceding it (*7*).

The initiation specificity of free primase in vitro is quite high for an RNA polymerase in that it initiates phosphodiester bond formation between ATP and GTP to create pppApG when it is bound to the trinucleotide sequence d(CTG) within the ssDNA template (*8*). This specificity can be contrasted with that of transcription RNA polymerase which initiates with ATP or GTP and any NTP. Once initiated, primer synthesis continues rapidly for about 12

† This work was supported by funds to L.P. from Utah State University and to M.A.G. from the Council for Tobacco Research, Inc. No. 3581, and the National Science Foundation OSR-9255225.

* Corresponding author. Tel: 402-472-3429. Fax: 402-472-9402. E-mail: mgriep@unlserve.unl.edu.

‡ Utah State University.

§ University of Nebraska.

10.1021/bi983059f CCC: $18.00
Published on Web 05/14/1999

nucleotides and then slows down so that primers 12 nucleotides and longer are observed. This length dependence is comparable to that observed in vivo (*9*). Magnesium is essential for primase activity and is probably used catalytically to form the phosphodiester bonds in the same way that it is used by other RNA and DNA polymerases (*10*, *11*).

Primase undergoes a dramatic conformational change at high magnesium acetate concentration (*12*). Limited tryptic digestion was used in a thermodynamic manner to determine that binding occurs with low cooperativity and involves at least two magnesiums. The low magnesium conformation is active, while the high magnesium is not. The conformational change is strongest when using magnesium acetate rather than magnesium chloride or sulfate, indicating a special role for the anion in the inhibitory conformational change. Analysis of the tryptic digestion pattern indicates that high magnesium somehow prevents trypsin cleavage at Arg110. There is a glutamate-rich sequence located between residues 80 and 100, and magnesium may bind to this anionic hinge to prevent trypsin access to adjacent position 110.

The functional domains of primase have been investigated by sequence analyses of primases and transcription RNA polymerases (*13*−*15*). The most highly conserved sequence in primases is a putative zinc-binding motif located at roughly residues 35−70 in the bacterial sequence. Indeed, there is one zinc bound per primase (*16*) which is not used catalytically but structurally (*17*). The bound zinc prevents inhibitory disulfide bond formation of the zinc-ligating cysteines (*17*). Proteins and enzymes that use zinc in a structural manner are ubiquitous throughout nature. These zinc proteins form distinct tertiary structural classes (*18*−*20*). These "structural" zincs are tetrahedrally bound by short protein sequences using two, three, or four cysteines and are called "zinc fingers". Interestingly, many of the classes of zinc fingers are involved in either specific or nonspecific nucleic acid binding. Since the role of the primase zinc site is to generate sequence specificity during polymer initiation (*21*, *22*), elucidating the structure and function of the zinc site in primase is critical to understanding primase structure and function. We report here X-ray absorption spectroscopy (XAS)[1] studies of the zinc in *E. coli* primase when the enzyme is either free or bound to its cofactors and substrates.

EXPERIMENTAL PROCEDURES

Primase Sample Preparation and Post-Irradiation Integrity. Primase was isolated and its activity quantitated according to standard protocols (*17*). Primase was transferred to a buffer of 50 mM HEPES, 50 mM KCl, pH 7.5, and concentrated to 1.0 mM using a Centricon-10 apparatus (Amicon, Beverly, MA), the indicated substrate concentration was added, and the sample was snap frozen in liquid nitrogen. Immediately before data collection, the sample was thawed, transferred to the plexiglass holder, and then frozen again in liquid nitrogen. Post-irradiation, the samples in the holders were thawed and then analyzed by SDS gel electrophoresis using a polyacrylamide gradient from 10% to 17% as previously described (*12*). Analysis of the Coomassie Blue-stained gel indicated that neither sample handling nor the intense X-ray beam altered the integrity of the single-chain primase.

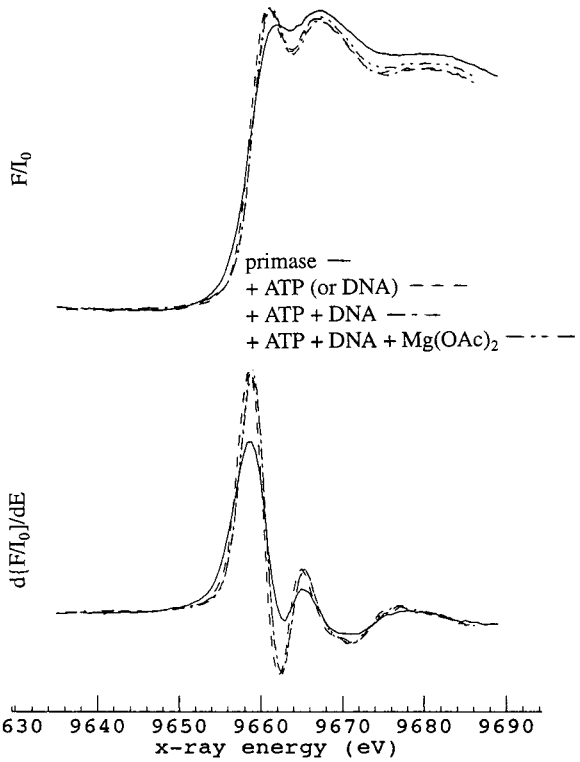

FIGURE 1: Normalized X-ray absorption edge spectra (a) and derivatives (b) for the zinc in primase ± 30 mM $Mg(OAc)_2$ ± 2 mM ATP ± 3 mM $(dT)_{17}$.

X-ray Absorption Measurements. X-ray absorption measurements were performed on Beamline X9 at the National Synchrotron Light Source using Si 111 crystals which provide ∼1 eV resolution at 9 keV. Protein samples and model compounds were maintained at ∼−80 °C during X-ray exposure to reduce the effects of radiation damage (*23*). A 13-element Ge detection system was used for fluorescence data collection. The spectra were collected and averaged until the signal-to-noise ratio at ∼10.3 keV ($k \sim 13$ Å^{-1}) was >2. The energy was calibrated using a Zn metal foil before and after each edge spectra giving an error of ±0.2 eV.

X-ray Absorption Data Analysis. The data were analyzed according to previously described methods (*24*−*30*). The edge data were normalized in the same manner as the EXAFS oscillations after the absorption below the edge region was set equal to 0 (Figures 1, 4).

The EXAFS modulations are described by the following:

$$\chi(k) = -\frac{1}{k^3}\sum_i \frac{N_i Z_i}{r_i^2} e^{-2\sigma_i^2 k^2} \sin\left[2kr_i + \alpha_i(k)\right]$$

where N_i is the number of neighboring atoms at distance r_i, Z is the atomic number of the scattering atoms, σ_i is the Debye−Waller factor describing thermal and lattice disorder, and $\alpha_i(k)$ is the phase shift due to the potentials of the absorbing and scattering atoms. The value of the wave vector k is given by $k = 2\pi[2m_e(E_{X-ray} - E_0)]^{1/2}/h$, where m_e is the rest mass of one electron and h is Planck's constant. Analysis of the data consists of background subtraction and normal-

[1] Abbreviations: HEPES, *N*-(2-hydroxyethyl)piperazine-*N*′-(2-ethanesulfonic acid); PMPS, *p*-hydroxymercuriphenylsulfonate; XAS, X-ray absorption spectroscopy.

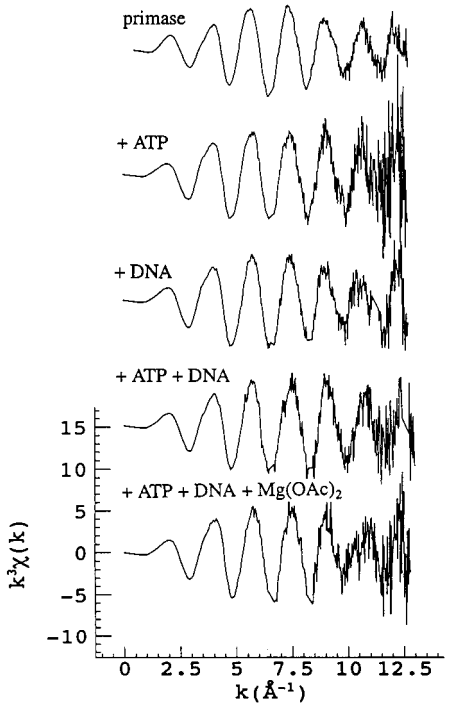

FIGURE 2: Extended X-ray absorption fine structure spectra for the zinc in primase ± 30 mM $Mg(OAc)_2$ ± 2 mM ATP ± 3 mM $(dT)_{17}$. The data were background-subtracted and then multiplied by k^3 to obtain the spectra shown.

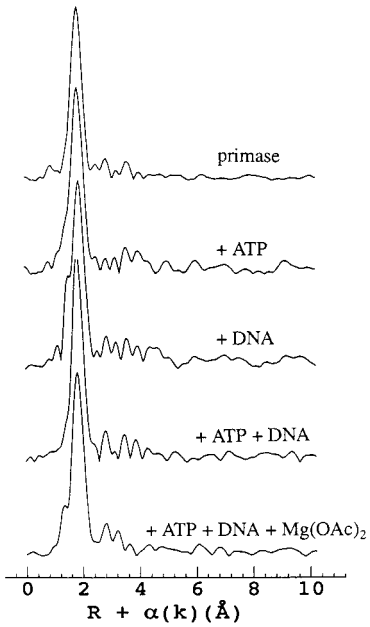

FIGURE 3: Fourier transforms of the data shown in Figure 2.

ization, k^3 multiplication which approximately equalizes the modulations in *k*-space (Figures 2, 5), and Fourier transformation which removes the summation (Figures 3, 6) and translates the data from energy space to position space. The contribution of each shell was isolated by application of a Fourier window filter and back-transformation. Thus, for each coordination shell *i*, the amplitude contains *N* and σ while the phase contains the average distance *r*. Comparison of the sample amplitude and phase with those of carefully chosen model compounds having similar structure and for which the structure has been determined gives the sample parameters *r*, *N*, $\Delta\sigma^2$, and ΔE_0, where $\Delta\sigma^2 = \sigma^2_{model} - \Delta^2_{protein}$ and $\Delta E_0 = E_{0,model} - E_{0,protein}$. The "goodness" of the fit was calculated by the sum of the residuals squared, ΣR^2. It was not necessary to divide this quantity by the number of data points in the fit because the number of data points was the same for all fits.

Table 1: Primase Zinc Two-Atom Fits When the Protein Is Either Free or Bound to Various Substrates[a]

Zn ligand	*r* (Å)	N	$\Delta\sigma^2$ ($\times 10^3$)	ΔE_o (eV)	ΣR^2
1 mM Free Primase					
S	2.36	3	0.34	2.4	3.2
N	2.15	1	2.1	−4.0	
1 mM Primase + 50 mM $Mg(OAc)_2$					
S	2.36	3	0.42	2.4	6.0
N	2.11	1	2.4	−3.5	
1 mM Primase + 2 mM ATP					
S	**2.35**	**3**	**0.94**	**2.8**	**5.2**
N	**2.14**	**2**	**−7.7**	**−1.8**	
S	2.35	3	0.95	2.2	5.1[b]
N	2.15	3	−12	−1.8	
1 mM Primase + 3 mM $(dT)_{17}$					
S	**2.36**	**3**	**2.0**	**3.4**	**4.1**
N	**2.05**	**2**	**−2.8**	**−1.6**	
S	2.36	3	1.8	3.3	5.9
N	2.05	3	−7.0	−1.6	
1 mM Primase + 2 mM ATP + 3 mM $(dT)_{17}$					
S	**2.33**	**3**	**−2.8**	**3.5**	**6.5**
N	**2.18**	**2**	**−2.2**	**−2.6**	
S	2.33	3	−4.8	2.9	7.6
N	2.183	−8.3	−2.4		
1 mM Primase + 30 mM $Mg(OAc)_2$ + 2 mM ATP + 3 mM $(dT)_{17}$					
S	**2.35**	**3**	**0.61**	**2.9**	**7.6**
N	**2.11**	**2**	**−5.7**	**−1.9**	
S	2.35	3	4.3	2.3	7.3
N	2.13	3	−9.5	−1.9	

[a] The one or two best solutions are shown for fits in which the number *N* of each type of atom was held constant during minimization. The metal-to-sulfur ligand distance measurements are precise to within 0.02 Å, metal to nitrogen/oxygen distance measurements are precise to within ±0.03 Å, the Debye−Waller disorder parameters $\Delta\sigma^2$ are accurate to within 30% of the standards zinc(imidazole)$_4$ and zinc(diethyldicarbamate)$_2$, and the differences between the fit and the actual edge energy ΔE_o are accurate to within 1.5 eV. [b] This best fit has an especially large Debye−Waller factor, $\Delta\sigma^2$.

To compare the results of the fitting procedure, we must determine how much the ΣR^2 values must differ for the fits to be considered statistically different. The number of degrees of freedom in the fit, ϕ_f, is related to the number of degrees of freedom in the data, ϕ_d, by $\phi_f = \phi_d - \nu$, where ν is the number of variable parameters in the fit. The value ϕ_d is calculated from $2\Delta w\Delta k/\pi$ where Δw is the full width at half-maximum or the normalized area of the window function and $\Delta k = k_{max} - k_{min}$. For the data presented here, $\Delta w = \sim 1.1$ Å and $\Delta k = \sim 13.0$ Å^{-1} which means that ϕ_d is 9.5 and ϕ_f is 3.5. Thus, the minimum criteria becomes $\Sigma R^2 > \Sigma R^2_{min}(1 + 1/\phi_f) \sim \Sigma R^2_{min}(1.3)$. The best solution(s) is(are) that(those) with ΣR^2_{min} which can be distinguished from other solutions by the above criteria and in which the parameters are physically reasonable (*24*−*30*).

Error estimation was obtained from the correlation and Hessian matrixes of the nonlinear least-squares fits and by varying each parameter in the fit with the others held constant until ΣR^2_{min} doubles on each side of the minimum. The fitting results reported in Table 1 have used these methods, and the best solutions as judged by these criteria are in bold type.

Note that data from $k \sim 0-12.5$ Å^{-1} was used in the analysis. When the site can be accurately modeled, by

compounds of similar chemical structure, data $k < \sim 4$ Å can be used with little error (*28*, *31*−*33*). For these data, fits were also compared for data $k > \sim 4$ Å, and no changes in the parameters were observed within the errors. An example of the best fit (Table 1) compared to the first shell-filtered data for free primase is shown in Figure 7 together with a comparison of the residuals with the estimated error. The residuals for the best fits for all of the data are comparable to the estimated error showing that the fits account for all of the data, but largely exclude the noise.

The Zn−N model compound was $Zn(imidazole)_4$ in aqueous solution which was prepared according to the methods of Mims and Piesach (*34*). The average Zn−N(imidazole) distance was determined by EXAFS analysis in comparison to tetraimidazole zinc(II) perchlorate powder (*35*, *36*) because it provided a better approximation to the protein ligand environment especially in the higher ligation shells. The Zn−S model compound was Zn(diethyldithiocarbamate)$_2$ (*37*).

There is often difficulty in determining the number of S and N ligands, due to the fact that the phases of S and N oscillations are nearly out of phase over a large portion of the data range. An example of these difficulties is given by Peisach (*38*) for the blue copper protein, stellacyanin, together with very conservative data analysis methods which expose the difficulties and address them. These methods were used in the analysis. Other examples have recently been presented by Clark-Baldwin (*39*).

RESULTS

The putative zinc-binding ligands of primase are the highly conserved residues (*13*). Because high sequence conservation is often a predictor of residues important for function, the primase zinc site has been an object of considerable study (*17*, *22*, *40*−*43*). Even though zinc is a spectrally reticent atom, X-ray absorption spectroscopy can be used to determine the ligands and their distances from the metal center. After preliminary XAS experiments showed that the primase zinc structure was sensitive to substrate binding, we undertook the following study of the primase zinc ligation states. This is the first study to demonstrate that the primase zinc ligation changes when the enzyme binds to its substrates.

Native Primase and Primase Bound to 30 mM Mg(OAc)$_2$. The K-edge X-ray absorption features (Figure 1) for native primase are consistent with tetrahedral zinc coordination (*32*, *44*). After the EXAFS spectrum was background-subtracted and k^3-multiplied (Figure 2), the data generally had a resolution of $\Delta r = \sim 0.1$ Å. After the EXAFS data was Fourier transformed (Figure 3), the data was fit to various combinations of S and N ligands totalling 4, 5, and 6. Only the best solutions are shown (Table 1). The results for native primase unambiguously indicated tetrahedral coordination by 3 S ligands at an average distance of 2.36 ± 0.02 Å and 1 N ligand at 2.15 ± 0.03 Å. Three sulfur ligands are in accord with previous chemical displacement (*17*) and cobalt substitution (*43*) studies. The N contribution can be further identified as a histidine since the imidazole nitrogens and carbons appropriate for a single histidine can be identified by their characteristic outer shell contributions (2.5−4 Å, Figure 3) (*30*, *45*).

When primase was bound to low magnesium acetate (50 mM), there was little if any change in the zinc edge, indicating no change in ligand coordination geometry compared to free primase. This is confirmed by the fact that the fitting parameters for the low magnesium acetate samples are within the errors of those for free primase (Table 1) as are the higher coordination shells. This amount of magnesium was more than sufficient for the full activity of primase ($[Mg(OAc)_2]_{optimum} = 10$ mM) (*7*) but not enough to cause the full metal-dependent conformational change ($K_{50\%} = \sim 40$ mM and a cooperativity factor of 2) (*12*). Thus, when magnesium binds only to the catalytic metal-binding site(s), it does not induce a structural change in the zinc-binding domain of primase.

Primase Bound to Its Substrates. When free primase is compared to that of primase bound to 2 mM ATP, little or no change in the edge energy is observed but the relative intensities of the features change significantly (Figure 1). This change is also observed when primase is bound to 3 mM $(dT)_{17}$ or to a combination of substrates such as 3 mM $(dT)_{17}$; ATP and $(dT)_{17}$; or ATP, $(dT)_{17}$, and low magnesium acetate. In every case, this is indicative of a change in the coordination state of the zinc site by comparison with model compounds (*44*).

Good fits of the first coordination shell data for primase bound to its substrates were obtained with 3 S ligands and either 2 or 3 N/O ligands (Table 1). While the higher shells still indicate the presence of a single histidine N ligand, they are changed significantly on binding substrates. These changes are clearly larger than the noise, indicating a change in coordination of the zinc site. Water can also be ruled out as the additional ligands since their hydrogen atoms would not be observed in the higher coordination shells. For all bound substrate combinations, our results show that one or two N/O ligands are added to the free primase structure. Except for the addition of ssDNA only, we cannot distinguish between the solutions having one or two additional ligands using the criteria discussed in the Experimental Methods section. However, solutions with a second additional ligand exhibit a large negative change in Debye Waller factor ($\Delta\sigma^2$), indicating that the second additional ligand is not bound as tightly as the first or the histidine nitrogen ligand of the free primase, even though the average bond length is not significantly changed. It is also worth noting that the addition of ssDNA also produces a $\Delta\sigma^2$ for the addition of an N/O ligand that is more negative than free primase. This implies that the additional ligands (whether one or two) are not bound the same as the histidine nitrogen ligand in free primase, with distances either shorter (e.g., primase + 3 mM $(dT)_{17}$) or longer (other substrate combinations). The average Zn−S distance to the 3 S for the 4 substrate combinations is 2.36 Å ± 0.02 Å, the same as that for the free primase. In all cases in which ATP was bound, the average N/O distances are essentially unchanged from that of native primase and within our conservative error estimate. When ssDNA was bound in the absence of the other substrates, an average N/O distance was observed that was significantly less than that in free primase, 2.05 ± 0.03 Å. Therefore, the substrates induced either what we term the "active" conformation or the "ssDNA-bound" conformation. The zinc site structure is very sensitive to substrates.

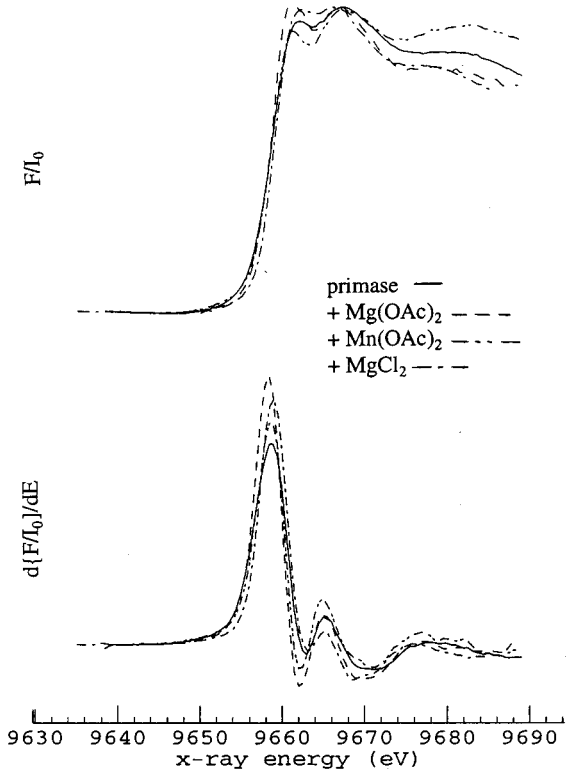

FIGURE 4: Normalized X-ray absorption edge spectra (a) and derivatives (b) for the zinc in free primase or in primase incubated with 300 mM of $Mg(OAc)_2$, $Mn(OAc)_2$, or $MgCl_2$.

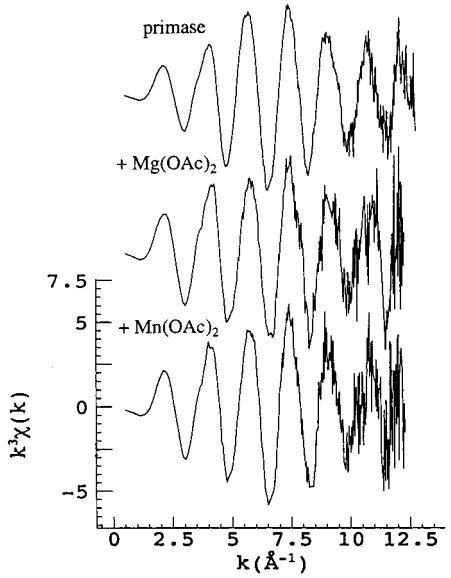

FIGURE 5: Extended X-ray absorption fine structure spectra for the zinc in free primase or in primase incubated with 300 mM $Mg(OAc)_2$, $Mn(OAc)_2$, or $MgCl_2$. The data were background-subtracted and then multiplied by k^3 to obtain the spectra shown.

The High Magnesium Acetate Primase Conformational Change. In recent studies using limited tryptic digestion, we found that high magnesium acetate caused a large perturbation in the primase conformation (*12*). In the presence of 300 mM $Mg(OAc)_2$, the zinc structure is changed (Figures 4, 5, 6, 7). One or two additional N/O ligands are bound, resulting in an average N/O ligand distance of 2.19 ± 0.03 (Table 2). Our previous study indicated that $MgCl_2$ and $MgSO_4$ were much less effective than $Mg(OAc)_2$ in causing this conformational change (*12*). When primase is incubated with high $MgCl_2$, the zinc edge structure (Figure 4) indicates that it is less changed compared to the free primase than that induced by high $Mg(OAc)_2$. Since these are identical for both $Mg(OAc)_2$ and $Mn(OAc)_2$ (Figure 6), it is likely

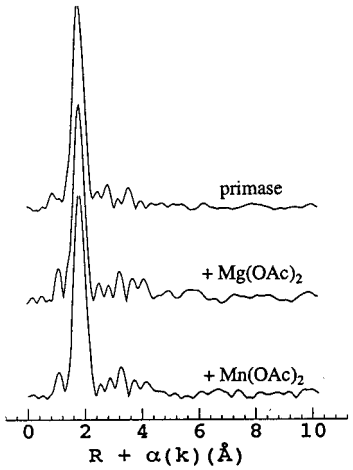

FIGURE 6: Fourier transforms of the data shown in Figure 5.

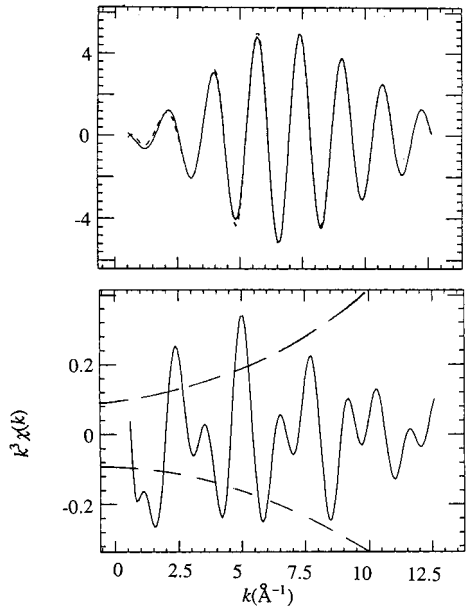

FIGURE 7: (top) Comparison of the first shell-filtered data for free primase (—) with the best fit in Table 1 (---). (bottom) Comparison of the residuals of the best fit in Table 1 for free primase (—) with our estimated error (---).

Table 2: Primase Zinc Two-Atom Fits When the Protein Is Either Free or Bound to High Concentrations of Selected Divalent Cations[a]

Zn ligand	r (Å)	N	$\Delta\sigma^2$ ($\times 10^3$ Å^2)	ΔE_o (eV)	ΣR^2
1 mM Free Primase					
S	2.36	3	0.34	2.4	3.2
N	2.15	1	2.1	−4.0	
1 mM Primase + 300 mM $Mg(OAc)_2$					
S	**2.34**	**3**	**−1.6**	**0.9**	**5.3**
N	**2.18**	**2**	**−1.7**	**−4.9**	
S	2.34	3	−1.6	0.4	6.5
N	2.20	3	−3.2	−4.8	
1 mM Primase + 300 mM $Mn(OAc)_2$					
S	2.37	3	0.16	0.9	4.8
N	2.12	1	3.7	−4.5	
S	**2.37**	**3**	**−1.3**	**0.3**	**4.2**
N	**2.15**	**2**	**−1.2**	**−4.3**	

[a] The legend is the same as in Table 1.

that the additional ligand(s) is(are) acetate anion(s) and changes observed in the higher order shell are consistent with this. This suggests an importance of the anion associated with magnesium and indicates that the acetate plays a structural role in the conformational change.

The Distance Between Zinc and the Catalytic Metal Site. To examine the distance between the catalytic metal and the zinc in primase, the zinc site was studied when the enzyme was incubated with high $Mn(OAc)_2$. Manganese has a larger atomic number than magnesium, which enhances the backscattering. Thus, it is likely to be observed if this site is close to the zinc site. The advantage is that, even though manganese can substitute for magnesium during catalysis, $Mn(OAc)_2$ does not cause the inhibitory conformational change (*12*).

When primase was incubated with high $Mn(OAc)_2$, the zinc site structure (Figures 4, 5, 6, Table 2) is changed but is different from that induced by high $Mg(OAc)_2$ (Table 2) and more similar to that of the free primase. One possible solution shows no change from free primase. This solution is less likely in view of the edge data (Figure 4) than the solution which shows an additional N/O ligand at essentially the same average distance as the histidine nitrogen of free primase. Furthermore, the higher shells differ from those of free primase. These are identical within the error to those induced by $Mg(OAc)_2$ (Figure 6), which suggests that the catalytic binding site is $> \sim 5$ Å from the zinc-binding site. It is also possible that the zinc and manganese are closer but are not observed due to large thermal/lattice disorder.

DISCUSSION

X-ray absorption spectroscopy has established that the *E. coli* primase zinc will adopt different ligation states when the enzyme is bound to its substrates, cofactors, or inhibitors. This demonstrates that the zinc-binding region of primase plays a critical role during primer synthesis and that the zinc is at or near the site of action. Taken in concert with the data of researchers on the same or homologous enzymes, our data suggest that there is communication between the zinc-binding and catalytic sites of primase which results in a major perturbation of the zinc ligation state.

Zinc Ligation. The zinc(II) edge features do not change much because its full $3d^{10}$ electronic configuration does not allow for much electron sharing or ligand field stabilization (*25*, *44*, *46*). Instead, the coordination number represents a balance between ligand bonding and repulsion energies resulting in a low-energy barrier between coordination to 4, 5, or 6 ligands (*47*, *48*). In fact, a number of zinc enzymes utilize these low-energy barriers between ligation states in their catalytic mechanisms (*49*). The consequence is that we rely on both the edge zinc X-ray absorption edge and EXAFS spectra to provide information about zinc ligation. Taken together, our results clearly show that the zinc site nitrogen/oxygen ligation increases by one or two ligands on binding substrates.

The Zn−S average distance as well as the Zn−N, O average distances are comparable to other reported zinc model compounds containing three S as well as N and O ligands (for example, see refs *50* and *51*).

Identifying the Primase Zinc Ligands. According to XAS, the free primase zinc site is tetrahedrally coordinated by three sulfur atoms at 2.36 ± 0.02 Å and one imidazole nitrogen at 2.15 ± 0.03 Å. This geometry and structure confirms and extends the predictions and observations made by primase amino acid sequence analysis (*14*), primase zinc removal studies (*17*), and primase zinc site peptide studies (*43*). The amino acid sequence analysis identified an amino-terminal sequence, Cys40-X_2-His43-X_{17}-Cys61-X_2-Cys64, similar, but not identical, to any known zinc-binding sequence. The homology of this sequence among bacterial primases predicted that the zinc is ligated by three cysteines and one histidine. No other cysteines or histidines are identical among the bacterial primases. Experimental evidence for this sequence prediction came from our zinc removal studies that indicated that there were three sulfur ligands to the zinc. Cobalt absorption studies of a peptide based on the *E. coli* primase zinc site sequence were consistent with tetrahedral coordination by three sulfur and one imidazole nitrogen. Taken together these results indicate that this sequence is the primase zinc-binding sequence.

When primase is bound by low magnesium acetate concentration, no changes are observed in the zinc site. However, when primase is inhibited by high magnesium acetate, the zinc site gains additional N/O ligands which are likely from acetate. The conformational change was cooperative with respect to magnesium acetate, had a $K_{50\%}$ of ~40 mM, and involved a change in accessibility to trypsin so that cleavage no longer occurred at Arg110, but at Lys34 and Lys56. Because Arg110 falls in a region of low sequence conservation that separates the highly conserved amino-terminal zinc-binding residues from the rest of the conserved residues, it may reside within a magnesium acetate-dependent hinge. Because Lys34 and 56 are located near or within the zinc finger residues, there should be a perturbation of the zinc structure when primase is bound to high $Mg(OAc)_2$. Our results clearly show this to be the case. Furthermore, high $Mn(OAc)_2$ produces similar changes in the zinc site. The primase structural change is induced most strongly by magnesium acetate and much less effectively with magnesium sulfate or chloride (*12*).

When primase is bound to ssDNA, the zinc site also gains additional nitrogen/oxygen ligands, but the average distance is shortened considerably. However, when primase is bound to ATP and other combinations of cofactors and ssDNA, additional N/O ligands are also added, but their average distances are on average the same as that of the histidine nitrogen in free primase and within our conservative error estimate. It is likely that these additional ligands are phosphate oxygens from ssDNA or ATP, since changes in the higher shells resemble those of the phosphate backbone of ssDNA and phosphates of nucleotides. If we consider an octahedral geometry that is produced from the binding of substrates, two adjacent oxygens, bonded to the zinc at 2.16 Å, are ~3.10 Å apart. We have examined the possibility that these oxygens are from the ssDNA template. The phosphate backbone of DNA was examined, but no combination of oxygen atoms with this spacing could be identified. We were able to locate appropriately spaced oxygens; for example, oxygen atoms on adjacent guanine bases are 3.15 Å apart. These results suggest that ssDNA binds with a single phosphate oxygen in agreement with our EXAFS results. It was also noted that this distance almost exactly matches the spacing between adjacent phosphate oxygens in a nucleoside

triphosphate. The conformation of ATP was investigated by energy minimization using Biograph software. We suggest that these phosphates would be capable of ligating the primase Zn site upon ATP binding. Our EXAFS results suggest that, in each case where ATP is a part of the substrate combination, it is the ATP which actually binds the primase Zn site. High magnesium and manganese acetate induced a structure similar to that when ATP was bound.

Other studies also suggest substrate binding to the zinc site. One of a series of ATP analogues with chemical cross-linking groups on the gamma phosphate was found to be able to cross-link to His43 of primase and still be functional in a primer synthesis assay (*52*). That is, the ATP analogue that was covalently bound to His43 was also able to bind to the active site. This same study found that other ATP analogues with gamma phosphate linkers could be attached to the region containing Lys211 to Lys241 which lies within the catalytic domain of primase (*53*) and to Lys528 which lies in the sequence-divergent tail. These workers interpreted this to mean that His43, Lys528, and the Lys211−241 region lie near one another in the folded protein structure. However, it is also possible that there is enough protein flexibility so that when the gamma phosphate of ATP is covalently bound to each of these sites, the other phosphate groups can bind to the active site. On the other hand, ATP or ssDNA binding to the catalytic domain may simply cause a change in the associated zinc-binding domain.

Communication between the Primase Domains. As an RNA polymerase, primase is capable of both initiation and elongation of RNA polymers. Mechanistically, initiation means that primase is able to bind two nucleoside triphosphates complementary to a particular single-stranded DNA template sequence and catalyze phosphodiester bond formation between those two nucleotides. Even though the detailed primase initiation mechanism has not been established yet, these zinc structure studies indicate that primase is capable of binding ATP in the absence of catalytic magnesium. Because the same was true for single-stranded DNA, it suggests that primase must have an unordered substrate-binding mechanism. Remarkably, this ability to bind the initiating nucleotide in the absence of either magnesium or template DNA has been observed for *E. coli* RNA polymerase (*54*, *55*), suggesting that this might be a mechanistic similarity for all primer and transcription RNA polymerases.

Bacterial primase is composed of three major domains: the amino-terminal zinc-binding domain, the central catalytic domain, and the carboxyl-terminal tail (*13*). The very tip of the tail has been shown to be essential for the enzyme's interaction with DnaB helicase (*56*). Only the length of the tail is conserved, suggesting that it plays primarily a structural role. If the catalytic core domain is functionally homologous with other nucleic acid polymerases, then it carries out the elongation reaction, which means it must be capable of binding catalytic magnesium, a primer−template complex, and a nucleoside triphosphate. The zinc-binding domain of the homologous bacteriophage T7 primase-helicase is important for primase initiation sequence specificity (*21*, *57*, *58*). It has not been fully established how this domain structurally achieves this specificity, but it has been shown that, when this protein lacks its zinc-binding domain, it will initiate RNA polymers without sequence specificity. This indicates that the zinc-binding domain probably does not bind the template and the two initiating nucleotides in a sequence-specific manner, but that it rather provides the appropriate hydrogen bond partners for the template and the initiating nucleotides. Our studies here indicate that, when single-stranded DNA and ATP bind to their respective binding sites in the catalytic domain, the interaction between the catalytic domain and the zinc-binding domain is altered in such a way that it reflects which of these two substrates are bound.

Our data indicate the initiating nucleotide orientation relative to the zinc and catalytic magnesium. There is no change in the XAS data for Mn compared to Mg, which means that the catalytic metal is most likely located more than about 5 Å from the zinc. Since the catalytic magnesium is hypothesized to make contact with the 3′-hydroxyl of the nucleotide being elongated, this means that the initiating nucleotide is probably also more than 5 Å away from the zinc, which is near the triphosphate part.

REFERENCES

1. Kornberg, A., and Baker, T. A. (1992) *DNA Replication*, 2nd ed., W. H. Freeman and Company, New York.
2. Marians, K. J. (1992) *Annu. Rev. Biochem. 61*, 673−719.
3. Kelman, Z., and O'Donnell, M. (1995) *Annu. Rev. Biochem. 64*, 171−200.
4. McHenry, C. S. (1991) *J. Biol. Chem. 266*, 19127−19130.
5. Wu, C. A., Zechner, E. L., Reems, J. A., McHenry, C. S., and Marians, K. J. (1992) *J. Biol. Chem. 267*, 4074−4083.
6. Zechner, E. L., Wu, C. A., and Marians, K. J. (1992) *J. Biol. Chem. 267*, 4045−4053.
7. Swart, J. R., and Griep, M. A. (1995) *Biochemistry 34*, 16097−16106.
8. Swart, J. R., and Griep, M. A. (1993) *J. Biol. Chem. 268*, 12970−12976.
9. Yoda, K.-y., Yasuda, H., Jiang, X.-W., and Okazaki, T. (1988) *Nucleic Acids Res. 16*, 6531−6546.
10. Pelletier, H., Sawaya, M. R., Kumar, A., Wilson, S., and Kraut, J. (1994) *Science 264*, 1891−1903.
11. Steitz, T. A., Smerdon, S. J., Jäger, J., and Joyce, C. M. (1994) *Science 266*, 2022−2025.
12. Urlacher, T. M., and Griep, M. A. (1995) *Biochemistry 34*, 16708−16714.
13. Griep, M. A. (1995) *Indian J. Biochem. Biophys. 32*, 171−178.
14. Ilyina, T. V., Gorbalenya, A. E., and Koonin, E. V. (1992) *J. Mol. Evol. 34*, 351−357.
15. Versalovic, J., and Lupski, J. R. (1993) *Gene 136*, 281−286.
16. Stamford, N. P. J., Lilley, P. E., and Dixon, N. E. (1992) *Biochim. Biophys. Acta 1132*, 17−25.
17. Griep, M. A., and Lokey, E. R. (1996) *Biochemistry 35*, 8260−8267.
18. Klug, A., and Schwabe, J. W. R. (1995) *FASEB J. 9*, 597−604.
19. Schmiedeskamp, M., and Klevit, R. E. (1994) *Curr. Opin. Struct. Biol. 4*, 28−35.
20. Vallee, B. L., and Auld, D. S. (1993) *Acc. Chem. Res. 26*, 543−551.
21. Bernstein, J. A., and Richardson, C. C. (1988) *Proc. Natl. Acad. Sci. U.S.A. 85*, 396−400.
22. Mendelman, L. V., Beauchamp, B. B., and Richardson, C. C. (1994) *EMBO J. 13*, 3909−3916.
23. Chance, B., Angiolillo, P., Yang, E., and Powers, L. (1980) *FEBS Lett. 112*, 178−182.
24. Lee, P., Citrin, P., Eisenberg, P., and Kincaid, B. (1981) *Rev. Mod. Phys. 53*, 769−806.
25. Powers, L. S. (1982) *Biochim. Biophys. Acta 683*, 1−38.
26. Powers, L., Sessler, J., Woolery, G., and Chance, B. (1984) *Biochemistry 23*, 5519−5523.
27. Chance, B., Fischetti, R., and Powers, L. (1983) *Biochemistry 22*, 3820−3829.

28. Chance, B., Powers, L., Ching, Y., Poulos, T. L., Schonbaum, G., Yamazaki, L., and Paul, K. G. (1984) *Arch. Biochem. Biophys. 2235*, 596−611.
29. Chance, M., Parkhurst, L., Powers, L., and Chance, B. (1986) *J. Biol. Chem. 261*, 5689−5692.
30. Powers, L., and Kincaid, B. (1989) *Biochemistry 28*, 4461−4468.
31. Sinclair, R., Yamazaki, I., Bumpus, J., Brock, B., Chang, C.-S., Albo, A., and Powers, L. (1992) *Biochemistry 31*, 4892−4900.
32. Wu, F., Huang, W.-J., Sinclair, R., and Powers, L. (1992) *J. Biol. Chem. 267*, 25560−25567.
33. Chen, D., and Powers, L. (1995) *J. Inorg. Chem. 58*, 245−253.
34. Mims, W., and Peisach, J. (1978) *J. Chem. Phys. 69*, 4921−4930.
35. Bear, C., Duggan, K., and Freeman, H. C. (1975) *Acta Crystyllogr., Sect. B 31*, 2713−2715.
36. Lin, S.-L., Stern, E., Kalb (Gilboa), A., and Zhang, Y. (1991) *Biochemistry 30*, 2323−2332.
37. Reddy, P. S., and Srinivasan, R. (1965) *J. Chem. Phys. 43*, 1404−1406.
38. Peisach, J., Powers, L., Blumberg, W., and Chance, B. (1982) *Biophys. J. 38*, 277−285.
39. Clark-Baldwin, K., Tierney, D., Nandakumar, G., Gruff, E., Kim, C., Berg, J., Koch, S., and Penner-Hahn, J. (1998) *J. Am. Chem. Soc. 120*, 8401−8409.
40. Hine, A. V., and Richardson, C. C. (1994) *Proc. Natl. Acad. Sci. U.S.A. 91*, 12327−12331.
41. Ziegelin, G., Linderoth, N. A., Calendar, R., and Lanka, E. (1995) *J. Bacteriol. 177*, 4333−4341.
42. Kusakabe, T., and Richardson, C. C. (1996) *J. Biol. Chem. 271*, 19563−19570.
43. Griep, M. A., Adkins, B. J., Hromas, D., Johnson, S., and Miller, J. (1997) *Biochemistry 36*, 544−553.
44. Yachandra, V., Powers, L., and Spiro, T. (1983) *J. Am. Chem. Soc. 105*, 6596−6604.
45. Powers, L., Chance, B., Ching, Y., and Angiolillo, P. (1981) *Biophys. J. 34*, 465−498.
46. Yachandra, V. (1995) *Methods Enzymol. 246*, 638−675.
47. Cotton, F., and Hanson, H. (1958) *J. Chem. Phys. 28*, 83−91.
48. Srinivasta, V. C., and Nigam, H. L. (1972−3) *Coord. Chem. Rev. 9*, 275−310.
49. Bertini, I., and Luchinat, C. (1994) in *Bioinorganic Chemistry* (Bertini, I., Gray, H. B., Lippard, S. J., and Valentine, J. S., Eds.) pp 37−106, University Science Books, Mill Valley, CA.
50. Harrison, P., Begley, M., and Kikabhi, T. (1986) *J. Chem. Soc., Dalton Trans.*, 929−938.
51. Gronlund, P., and Wacholtz, W. (1995) *Acta Chrystallogr., Sect. C 51*, 1540−1543.
52. Mustaev, A. A., and Godson, G. N. (1995) *J. Biol. Chem. 270*, 15711−15718.
53. Sun, W., Tormo, J., Steitz, T. A., and Godson, G. N. (1994) *Proc. Natl. Acad. Sci. U.S.A. 91*, 11462−11466.
54. Wu, C. W., and Goldthwait, D. A. (1969) *Biochemistry 8*, 4450−4458.
55. Wu, C. W., and Goldthwait, D. A. (1969) *Biochemistry 8*, 4458−4464.
56. Tougu, K., and Marians, K. J. (1996) *J. Biol. Chem. 271*, 21391−21397.
57. Kusakabe, T., and Richardson, C. C. (1997) *J. Biol. Chem. 272*, 5943−5951.
58. Kusakabe, T., Baradaran, K., Lee, J., and Richardson, C. C. (1998) *EMBO J. 17*, 1542−1552.

BI983059F